Journal of The Electrochemical Society, **157** (9) A1026-A1029 (2010)
0013-4651/2010/157(9)/A1026/4/$28.00 © The Electrochemical Society

Aspects of the Surface Layer Formation on $Li_{1+x}Mn_2O_{4-\delta}$ during Electrochemical Cycling

F. Simmen,[a] A. Hintennach,[a] M. Horisberger,[b] T. Lippert,[a,z] P. Novák,[a] C. W. Schneider,[a] and A. Wokaun[a]

[a]General Energy Research Department and [b]Laboratory for Developments and Methods, Paul Scherrer Institut, CH-5232 Villigen PSI, Switzerland

The formation of a solid electrolyte interphase (SEI)-type layer on $Li_{1.05}Mn_2O_{3.96}$ films prepared by pulsed laser deposition on Pt coated p-doped silicon and cycled in 1 M $LiClO_4$ in propylene carbonate is reported. The formation of the SEI was studied as a function of the voltammetric charging/discharging sweep rate at 40°C in the potential range of 3.5–4.4 V vs Li/Li^+ using high resolution scanning electron microscopy and energy-dispersive X-ray spectroscopy. By applying an asymmetric charging/discharging cycle, it is possible to enhance the SEI layer formation. The observed cycling dependence of the SEI is indicative of a continuous formation and degradation process of the SEI depending on the cycling direction and the sweep rate.
 [DOI: 10.1149/1.3464798]

Manuscript submitted April 6, 2010; revised manuscript received June 23, 2010. Published July 26, 2010.

The spinel $LiMn_2O_4$ is a potential candidate as an electrode material for rechargeable lithium-ion batteries. It is easy and cheap to prepare the material with the advantage of being nontoxic as compared to $LiCoO_2$. A comparatively high irreversible charge capacity is however considered to be not favorable for technical applications. The irreversibility in the charging properties occurs, e.g., due to manganese dissolution and the formation of an additional layer. This is a so-called solid electrolyte interphase (SEI)-type layer on the positive electrode, thereby increasing the impedance of this electrode. An SEI can be formed by the electrolyte decomposition products within a defined potential range. The decomposition products can either consist of inorganic compounds (Li_2CO_3,[1,2] LiF,[1,3] Li_xPF_y,[1,3,4] $Li_xPF_yO_z$ [1,3,4]) and/or be the result of a polymerization of organic solvent molecules[5,6] such as polyethers[3] and polycarbonates/alkylcarbonates.[1-4,7]

The existence and formation of an additional layer is well known for negative electrode materials[8-14] and was also reported for positive, cycled electrodes.[1,15,16] This additional layer was termed SEI because it behaves like an additional layer between the metal electrode and electrolyte with similar properties like a solid electrolyte. Earlier work on the SEI formation was done, e.g., on carbonaceous material characterized by X-ray photoemission spectroscopy (XPS)[8,9] and time of flight secondary-ion mass spectrometry (TOF-SIMS)[8] to study the influence of the graphite planes on the SEI formation. The formation of an SEI on a negative electrode has advantages such as a substantial reduction in the capacity fading rate.[10] A recent overview on studies of the SEI formation on positive and negative electrodes is given in Ref. 11. The thickness of SEI layers on negative electrodes is up to several tens of nanometers; the SEI-type layers on positive electrodes, however, are only a few nanometers thick.[15] Therefore, the choice of appropriate characterization techniques, in particular in situ characterization, is limited to methods such as ^{7}Li NMR,[17] XPS,[3,18] Fourier transform IR,[2,5,19,20] ellipsometry,[16] Raman microscopy,[16] X-ray absorption fine structure,[21] and TOF-SIMS.[21] In addition, air sensitivity of the electrode/electrolyte interface is a limiting factor for the detection of the formed SEI.[22] Likewise, storage time, cycling conditions, and cycling temperature influence the thickness of the SEI layer.[18]

The goal of our work was to study the formation and behavior of the SEI on $LiMn_2O_4$ in detail without the influence of the carbon black or binder present in a standard composite electrode. Thus, it was necessary to use thin films as model electrodes. Thin films of $Li_{1+x}Mn_2O_{4-\delta}$ have been prepared by pulsed laser deposition (PLD),[23-27] radio-frequency magnetron sputtering,[28,29] electron-beam evaporation,[29,30] and electrostatic spray deposition.[31] For our studies, well-defined thin $Li_{1+x}Mn_2O_{4-\delta}$ films were grown on Pt coated silicon by PLD. The focus was on the influence of the cycling conditions on the SEI formation.

[z] E-mail: thomas.lippert@psi.ch

Experimental

Spinel film preparation and structural characterization.— Thin films of $LiMn_2O_4$ with a nominal composition of $Li_{1+x}Mn_2O_{4-\delta}$ were prepared on p-doped (100)-oriented silicon substrates by PLD (λ = 248 nm, F = 2.6 J cm^{-2}, 10 Hz). The substrate was coated before deposition with an additional ≈10 nm thick metallic layer of Pt by dc magnetron sputtering [TIPSI, 50 W (Pt), PK75 target, argon, 0.003 mbar]. The rodlike target was prepared by mixing $Li_{1.03}Mn_2O_4$ (99.7% purity, Honeywell) with an excess of 2.5 mol % Li_2O (99.5%, Alfa Aesar) to compensate for the Li loss during the deposition. Deposition took place in 0.2 mbar O_2 atmosphere at a deposition temperature T_s = 500°C and a substrate-target distance of 4 cm. After the deposition, the $Li_{1+x}Mn_2O_{4-\delta}$ thin films were cooled to room temperature with typical thicknesses for all investigated films of ~300 nm.

To precisely determine the film composition after the deposition, Rutherford backscattering and elastic recoil detection analysis were used. Information about the crystallinity was obtained by an X-ray diffractometer (Siemens D-500, Cu Kα) and the surface morphology before and after cycling was studied by a high resolution scanning electron microscope (SEM, Zeiss Supra VP55, in-lens detector, 3 kV). In addition, the spinel thin-film composition before and after electrochemical cycling was independently determined by an energy-dispersive X-ray (EDX) spectroscope (Zeiss Ultra, EDAX, Ametek EDX detector, 20 kV) to identify electrochemically induced changes to the film composition.

Electrochemical characterization.— Standard electrochemical cells were assembled in a glove box (H_2O < 0.1 ppm, O_2 ≈ 0.6 ppm). $Li_{1+x}Mn_2O_{4-\delta}$ film electrodes were used as the positive electrode and Li metal (Aldrich) as the counter electrode. Electrode separation was accomplished by a 1 mm thick glass fiber separator. The electrolyte was 1 M $LiClO_4$ in propylene carbonate (PC, Ferro). All electrochemical measurements were conducted in a potential range between 3.5 and 4.4 V vs Li/Li^+ at 40(±0.1)°C. The cells were disconnected at 4.0 V during the charging half-cycle and then dismantled and analyzed. Several oxidation and reduction sweep rates were applied (0.025, 0.05, and 0.1 mV cm^{-1}). Depending on the cycling conditions, the cells were run for 6 and 12 cycles. After cycling, the cells were disassembled in the glove box. Then the spinel films were washed with pure PC and subsequently dried in an argon atmosphere.

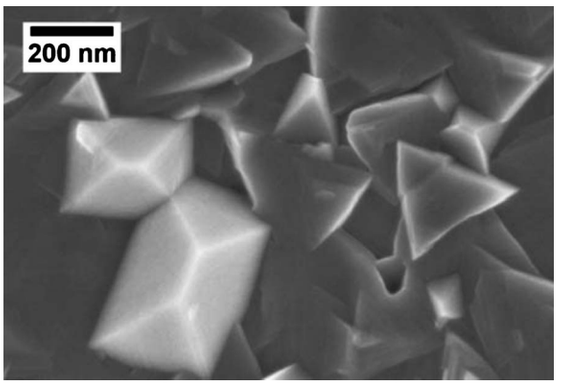

Figure 1. Surface morphology of a pristine thin spinel film deposited on Pt coated p-Si.

Results and Discussion

The average composition of ca. 300 nm thick films was $Li_{1.05}Mn_2O_{3.96}$. The films showed a lithium deficiency of 2.8% compared to the nominal target composition of $Li_{1.08}Mn_2O_{4.03}$ and an oxygen deficiency of 1.7%. The lithium deficiency could be due to a noncongruent transfer process during PLD caused by the collision and scattering of the light lithium by heavier elements in the plasma or by the oxygen background gas molecules and/or by sputtering/backscattering of the volatile lithium from the growing film.[32-34] The as-deposited $Li_{1.05}Mn_2O_{3.96}$ thin films on (100) Si are polycrystalline with a preferred (111) orientation and no detectable impurity phases. All films showed a regular surface morphology consisting of octahedral and tetrahedral crystallites (Fig. 1) with a surface roughness of 33 ± 7 nm (root-mean-square), determined with an area of 50×50 μm.

The $Li_{1.05}Mn_2O_{3.96}$ thin films were charged and discharged by cyclovoltammetry to study the influence of the sweep rate and cycle numbers on the formation of an additional layer, the SEI, on the surface of the cathode material. The cyclovoltammograms for all films showed the expected double peak structure characteristic for a two-step deinsertion process during charging (oxidation) and a two-step insertion process of the Li ions during the discharging (reduction) (Fig. 2a).

The electrochemical cells were cycled with selected sweep rates including asymmetric charging/discharging cycles to determine the influence of the kinetics on the formation of the SEI. It was assumed that an SEI is formed as a result of a decomposition process of the electrolyte at the spinel–electrolyte interface. In addition, a possible dissolution of $LiMn_2O_4$ gives rise to a loss of manganese beneath the SEI. The dissolution can be written as follows (Hunter equation)

$$2Mn^{3+}_{solid} \rightarrow Mn^{4+}_{solid} + Mn^{2+}_{solution} \quad [1]$$

These decomposition processes were expected to increase with increasing cycle numbers. The dependency of the sweep rate on the current density vs charging/discharging voltage is shown in Fig. 2a. For a defined sweep rate (symmetric charging/discharging), the observed systematic reduction in the current density with cycle numbers can be associated with aging of the electrode and the formation of the additional surface layer. Detailed SEM studies of the cycled spinel electrodes were performed and typical examples are shown in Fig. 2b-d. Two features on these electrode surfaces were noted with respect to untreated, noncycled spinel surfaces. Qualitatively, the overall surface roughness of the $Li_{1.05}Mn_2O_{3.96}$ thin film increases after cycling as a result of the electrochemical treatment and a pronounced crack formation appears. In addition, with decreasing sweep rates the ratio of the electrochemically altered to the not affected spinel surface becomes larger, as can be estimated from the respective SEM images. Furthermore, the amount of peeled off spinel film as well as the widths of the formed cracks increases with decreasing sweep rates. The formed layer appears to be of a soft consistency because it can be easily scratched using an atomic force microscope Si tip in contact mode without damaging the spinel surface.

What are likely the reasons for the described changes to the thin-film electrodes? Volumetric changes during charging and discharging take place, giving rise to an insertion induced stress.[35,36]

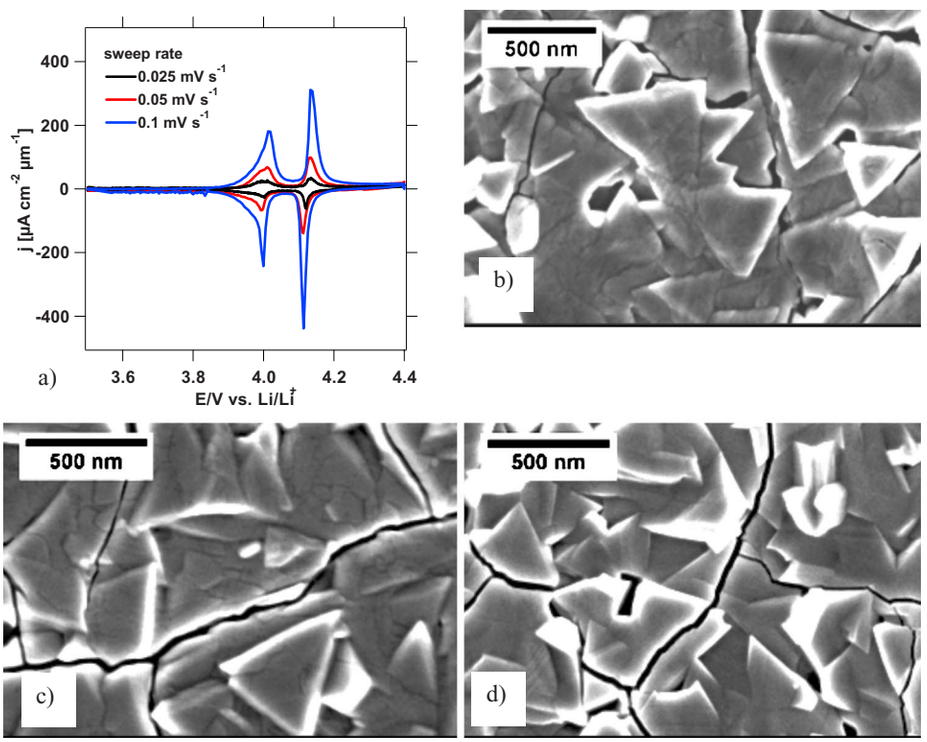

Figure 2. (Color online) (a) Typical cyclovoltammograms of $Li_{1.05}Mn_2O_{3.96}$ thin films in 1 M $LiClO_4$ PC electrolyte for different sweep rates (first cycle). [(b)-(d)] Surface morphology of $Li_{1+x}Mn_2O_{4-\delta}$ thin films cycled for six cycles with a sweep rate of (b) 0.025, (c) 0.05, and (d) 0.1 mV s^{-1}.

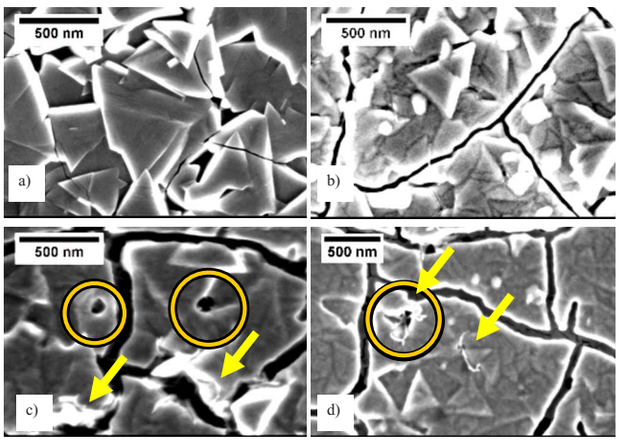

Figure 3. (Color online) Surface morphology of $Li_{1.05}Mn_2O_{3.96}$ thin films cycled with different sweep rates (oxidation–reduction sweep rate): For six cycles with (a) 0.025–0.1 mV s^{-1} and (b) 0.1–0.025 mV s^{-1}. For 12 cycles with (c) 0.025–0.025 mV s^{-1} and (d) 0.025–0.1 mV s^{-1}. The holes in the spinel layer are highlighted with circles and additional structures are marked with arrows.

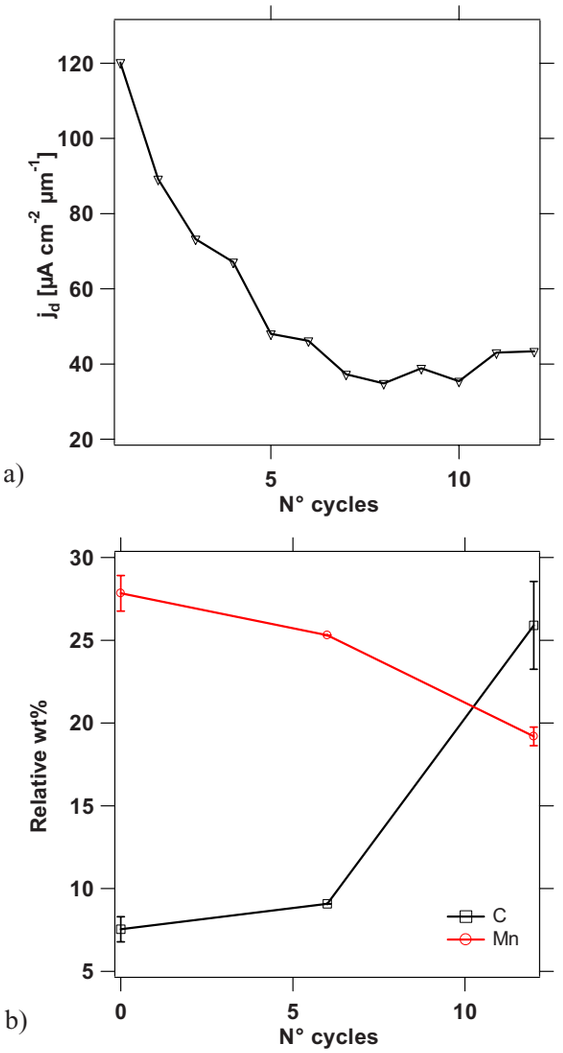

Figure 4. (Color online) (a) Normalized peak current density j_d during charging vs number of cycles and (b) evolution of the relative amounts of carbon and Mn at $Li_{1.05}Mn_2O_{3.96}$ electrodes cycled with an asymmetric sweep rate of 0.1–0.025 mV s^{-1}, as measured by EDX.

These volume changes are of the order 3–4%. It is also conceivable that a CO_2 evolution, while charging the electrochemical cell, further increases the already present mechanical stress in these films.[37] As a result, crack formation in the spinel develops and the adhesion between the film and substrate is reduced, which finally causes a peeling off of the spinel. The latter effect is visible during the dismantling of the cycled cell and the subsequent washing and drying process. The crack formation is also correlated with the sweep rate. For a sweep rate of 0.025 mV cm^{-1}, the most prominent crack formation is noted, indicative of an increased stress due to the enhanced interaction time.

The formation of the additional SEI layer shows a distinct time dependence. With lower charging and discharging rates, the decomposition process of the electrolyte, including possible side and follow-up reactions while on the reduction branch of the cycle, becomes more distinct (Fig. 3). This is particularly obvious by comparing the surfaces of films cycled with 0.1/0.1 and 0.1/0.025 mV s^{-1} for the respective charging/discharging cycles (Fig. 2d and 3b). The latter surface becomes very rough and the crack formation more pronounced, including softening of the edges. For a sweep rate of 0.05 mV s^{-1}, the additional SEI layer was sensitive to electron-beam irradiation as compared to samples cycled with 0.025 mV s^{-1}. This strongly suggests a change in composition of the SEI layer with respect to the cycling conditions.

What is the influence of the sweep rate during the oxidation and reduction processes on the formation of the SEI? As already pointed out, the fraction of the SEI layer decreases if for symmetric cycling conditions the sweep rate increases. This is consistent with a reduced interaction time for chemical reactions to take place at the SEI (Fig. 2). Applying asymmetric charging/discharging cycles, a noticeable increase in the observable SEI layer coverage can be obtained by applying a faster oxidation and a slower reduction rate. An example for the changes in surface modifications after six completed cycles using 0.1/0.025 mV s^{-1} for the charging and discharging sweep rate is shown in Fig. 3b. The surface becomes markedly changed with respect to pristine surfaces and the edges of the formed cracks show clear signs of corrosion. Studying the $Li_{1.05}Mn_2O_{3.96}$ surfaces after 12 completed cycles, corrosion effects are even more pronounced like a distinct hole formation not present for pristine spinel films (Fig. 3c and d, encircled). In severe cases, the thin spinel electrode was corroded such that the spinel layer was not electrochemically active any longer. This was also noted in cyclovoltammograms, where the characteristic double peak structure disappeared well before reaching the 12th cycle.

Cycling the cell with 0.1 and 0.025 mV s^{-1} for the charging and discharging sweep rate, respectively, the oxidative peak current density decreases strongly to ~36% of its starting value after 12 cycles (Fig. 4a). Likely reasons for this dramatic decrease in current density are (*i*) a loss of electrical contact due to peeled off film, (*ii*) aging of the material, and/or (*iii*) the formation of an additional blocking layer at the surface of the electrode. Studying the carbon coverage vs sweep rate and the composition of the spinel using EDX, the relative amount of carbon-containing species in the SEI layer increases significantly with increasing number of cycles (see Fig. 4b). Here, the carbon formation is assumed to be indicative for reaction products of the electrode and the electrolyte, i.e., for the SEI. The data indicate a decomposition of the electrolyte (i.e., formation of carbon-containing species) for small cycle numbers that increases dramatically for more than 6 cycles. The strong increase in carbon coincides with a significant decrease in Mn. A similar conclusion can be drawn from XPS measurements on samples cycled symmetrically with a sweep rate of 0.05 mV s^{-1} and stopped at a

potential of 4.0 V. Likewise, the amount of carbon increases and Mn decreases with increasing number of cycles.[38] Compared to the amount of carbon found for pristine samples due to air contamination (e.g., Li_2CO_3 and/or adsorbed carbon-containing species), spinel films cycled at low sweep rates showed an increase in the carbon content of 11–18%. For samples cycled with asymmetric charging/discharging cycles, an increase of up to 26–28% has been noted. In addition, a clear reduction of the relative amount of Mn in the electrode with increasing cycle numbers has also been measured (Fig. 4b). This is consistent with the already described corrosion of surfaces and cracks of the spinel electrodes (Fig. 3).

Conclusion

$Li_{1.05}Mn_2O_{3.96}$ thin films prepared by PLD showed the expected Li-ion deinsertion and insertion properties during charging and discharging cycles. The formation of an SEI-type layer takes place on thin-film model electrodes. The SEI formation is directly correlated with the number of charging and discharging cycles as well as the sweep rate. An important observation is that for faster sweep rates, the measurable fraction of an SEI-type layer on the electrode surface was less visible and detectable as compared to an SEI formation with slower cycling rates.

Acknowledgment

We thank all members of the Materials and Batteries Groups (PSI Villigen), Marc Mallepell, and Dr. Max Döbeli (ETH Zurich) for their support and measurements. The financial support of the Swiss National Science Foundation (SNF) is gratefully acknowledged.

References

1. A. M. Andersson, D. P. Abraham, R. Haasch, S. MacLaren, J. Liu, and K. Amine, *J. Electrochem. Soc.*, **149**, A1358 (2002).
2. C. Wu, Y. Bai, and F. Wu, *J. Power Sources*, **189**, 89 (2009).
3. T. Eriksson, A. M. Andersson, A. G. Bishop, C. Gejke, T. Gustafsson, and J. O. Thomas, *J. Electrochem. Soc.*, **149**, A69 (2002).
4. T. Eriksson, A. M. Andersson, C. Gejke, T. Gustafsson, and J. O. Thomas, *Langmuir*, **18**, 3609 (2002).
5. D. Ostrovskii, F. Ronci, B. Scrosati, and P. Jacobsson, *J. Power Sources*, **103**, 10 (2001).
6. J. Thevenin, *J. Power Sources*, **14**, 45 (1985).
7. M. Matsui, K. Dokko, and K. Kanamura, *J. Power Sources*, **177**, 184 (2008).
8. V. Eshkenazi, E. Peled, L. Burstein, and D. Golodnitsky, *Solid State Ionics*, **170**, 83 (2004).
9. E. Peled, D. B. Tow, A. Merson, A. Gladkirch, L. Burstein, and D. Golodnitsky, *J. Power Sources*, **97–98**, 52 (2001).
10. E. Strauss, D. Golodnitsky, and E. Peled, *Electrochim. Acta*, **45**, 1519 (2000).
11. P. B. Balbuena and Y. Wang, *Lithium Ion Batteries-Solid Electrolyte Interphase*, London Imperial College Press, London (2004).
12. J. O. Besenhard, M. Winter, J. Yang, and W. Biberacher, *J. Power Sources*, **54**, 228 (1995).
13. M. Lu, H. Cheng, and Y. Yang, *Electrochim. Acta*, **53**, 3539 (2008).
14. S. Leroy, H. Martinez, R. Dedryvère, D. Lemordant, and D. Gonbeau, *Appl. Surf. Sci.*, **253**, 4895 (2007).
15. M. Jo, Y.-S. Hong, J. Choo, and J. Cho, *J. Electrochem. Soc.*, **156**, A430 (2009).
16. J. Lei, L. Li, R. Kostecki, R. Muller, and F. McLarnon, *J. Electrochem. Soc.*, **152**, A774 (2005).
17. Y. Wang, X. Guo, S. Greenbaum, J. Liu, and K. Amine, *Electrochem. Solid-State Lett.*, **4**, A68 (2001).
18. K. Edstrom, T. Gustafsson, and J. O. Thomas, *Electrochim. Acta*, **50**, 397 (2004).
19. D. Aurbach, K. Gamolsky, B. Markovsky, G. Salitra, Y. Gofer, U. Heider, R. Oesten, and M. Schmidt, *J. Electrochem. Soc.*, **147**, 1322 (2000).
20. N. Liu, H. Li, Z. Wang, X. Huang, and L. Chen, *Electrochem. Solid-State Lett.*, **9**, A328 (2006).
21. H. Ota, T. Akai, H. Namita, S. Yamaguchi, and M. Nomura, *J. Power Sources*, **119–121**, 567 (2003).
22. R. Dedryvère, H. Martinez, S. Leroy, D. Lemordant, F. Bonhomme, P. Biensan, and D. Gonbeau, *J. Power Sources*, **174**, 462 (2007).
23. S. B. Tang, M. O. Lai, and L. Lu, *Mater. Chem. Phys.*, **111**, 149 (2008).
24. S. B. Tang, M. O. Lai, and L. Lu, *J. Alloys Compd.*, **449**, 300 (2008).
25. F. Simmen, T. Lippert, P. Novák, B. Neuenschwander, M. Döbeli, M. Mallepell, and A. Wokaun, *Appl. Phys. A: Mater. Sci. Process.*, **93**, 711 (2008).
26. F. Simmen, T. Lippert, P. Novák, B. Neuenschwander, M. Döbeli, M. Mallepell, and A. Wokaun, *Appl. Surf. Sci.*, **255**, 5303 (2009).
27. T. Doi, M. Inaba, Y. Iriyama, T. Abe, and Z. Ogumi, *J. Electrochem. Soc.*, **155**, A20 (2008).
28. C. C. Chen, K. F. Chiu, K. M. Lin, H. C. Lin, C. R. Yang, and F. M. Wang, *Phys. Scr.*, **T129**, 74 (2007).
29. S. W. Jin and H. N. G. Wadley, *J. Vac. Sci. Technol.*, **26**, 114 (2008).
30. V. K. Vani and O. M. Hussain, *AIP Conf. Proc.*, **1004**, 58 (2008).
31. K. Dokko, N. Anzue, M. Mohamedi, T. Itoh, and I. Uchida, *Electrochem. Commun.*, **6**, 384 (2004).
32. T. Dumont, T. Lippert, M. Dobeli, H. Grimmer, J. Ufheil, P. Novák, A. Wursig, U. Vogt, and A. Wokaun, *Appl. Surf. Sci.*, **252**, 4902 (2006).
33. D. O'Mahony, J. Lunney, T. Dumont, S. Canulescu, T. Lippert, and A. Wokaun, *Appl. Surf. Sci.*, **254**, 811 (2007).
34. S. Canulescu, E. L. Papadopoulou, D. Anglos, T. Lippert, C. W. Schneider, and A. Wokaun, *J. Appl. Phys.*, **105**, 063107 (2009).
35. I. Uchida, H. Fujiyoshi, and S. Waki, *J. Power Sources*, **68**, 139 (1997).
36. X. Zhang, A. M. Sastry, and W. Shyy, *J. Electrochem. Soc.*, **155**, A542 (2008).
37. M. Holzapfel, A. Wursig, W. Scheifele, J. Vetter, and P. Novak, *J. Power Sources*, **174**, 1156 (2007).
38. F. Simmen, A. Foelske, P. Verma, M. Horisberger, T. Lippert, P. Novák, and A. Wokaun, Unpublished.